3,5-Di-C-β-$_D$-glucopyranosyl phloroacetophenone, a major component of *Melicope ptelefolia*, suppresses fibroblast activation and alleviates arthritis in a mouse model: Potential therapeutics for rheumatoid arthritis

HYUN JONG KIM[1], JI HYUN CHOI[1,2], JUNG-HWAN HWANG[1,2], KYONG-SHIM KIM[1,2], JUNG-RAN NOH[1], DONG-HEE CHOI[1], SUNG JE MOON[1], HYUN-YONG KIM[1], SANG-WOO KIM[3], SANGHO CHOI[4], SANG MI EUM[4], TRAN THE BACH[5], JAERANG RHO[6], JU YONG LEE[7], JUNG GEUN PARK[7], SEI-RYANG OH[2,8], CHUL-HO LEE[1,2], WON KEUN OH[7] and YONG-HOON KIM[1,2]

[1]Laboratory Animal Resource Center, Korea Research Institute of Bioscience and Biotechnology, Daejeon 34141; [2]University of Science and Technology, Daejeon 34113; [3]Laboratory Animal Center, Osong Medical Innovation Foundation, Cheongju, Chungcheongbuk-do 28160; [4]International Biological Material Research Center, Natural Medicine Research Center, Korea Research Institute of Bioscience and Biotechnology, Daejeon 34141, Republic of Korea; [5]Institute of Ecology and Biological Resources, Vietnam Academy of Science and Technology, Hanoi, Vietnam; [6]Department of Microbiology and Molecular Biology, Chungnam National University, Daejeon 34134; [7]Korea Bioactive Natural Material Bank, Research Institute of Pharmaceutical Sciences, College of Pharmacy, Seoul National University, Seoul 08826; [8]Natural Medicine Research Center, Korea Research Institute of Bioscience and Biotechnology, Daejeon 34141, Republic of Korea

Received May 3, 2018; Accepted August 28, 2018

DOI 10.3892/ijmm.2018.3849

Abstract. *Melicope ptelefolia* has been traditionally used to treat rheumatism and fever. The present study aimed to investigate the therapeutic effect of 3,5-di-C-β-$_D$-glucopyranosyl phloroacetophenone (βGP), a main component of *M. ptelefolia*, on rheumatoid arthritis (RA). A model of collagen-induced arthritis (CIA) was established in mice using the RAW 264.7 murine macrophage cell line and mouse embryonic fibroblasts (MEFs). The clinical scores of arthritis, swelling, histopathological findings, and micro-computed tomography in CIA mouse paws were assessed. The levels of anti-type II collagen antibody and cytokines were determined in the plasma and cell culture supernatant, respectively. Protein and gene expression levels were analyzed by western blot and reverse transcription-quantitative polymerase chain reaction analyses. βGP significantly decreased the gross arthritic scores of CIA mice and joint swelling, and decreased articular inflammation, cartilage degradation and bone erosion. However, βGP did not exert any effect on anti-type II collagen immunoglobulin G plasma levels or inflammatory cytokine expression in macrophages. βGP significantly suppressed the expression of interleukin-6 and leukemia inhibitory factor and decreased the phosphorylation of signal transducer and activator of transcription 3, and expression of receptor activator of nuclear factor-κB ligand in tumor necrosis factor-α-stimulated MEFs and in CIA mouse paws. Osteoclast-related gene expression was significantly reduced in CIA mouse paws. Taken together, βGP suppressed the development of RA by regulating the activation of synovial fibroblasts.

Correspondence to: Professor Won Keun Oh, Korea Bioactive Natural Material Bank, Research Institute of Pharmaceutical Sciences, College of Pharmacy, Seoul National University, 1 Gwanak-ro, Gwanak-gu, Seoul 08826, Republic of Korea
E-mail: wkoh1@snu.ac.kr

Dr Yong-Hoon Kim, Laboratory Animal Resource Center, Korea Research Institute of Bioscience and Biotechnology, University of Science and Technology, 125 Gwahak-ro, Yuseong-gu, Daejeon 34141, Republic of Korea
E-mail: yhoonkim@kribb.re.kr

Abbreviations: βGP, 3,5-di-C-β-$_D$-glucopyranosyl phloroacetophenone; CIA, collagen-induced arthritis; H&E, hematoxylin and eosin; *M. ptelefolia, Melicope ptelefolia*; MPPE, Melicope ptelefolia ethanol extract; μCT, micro-computed tomography; MEFs, mouse embryonic fibroblasts; RANKL, receptor activator of nuclear factor-κB ligand; RA, rheumatoid arthritis; Th, T helper

Key words: 3,5-di-C-β-$_D$-glucopyranosyl phloroacetophenone, collagen-induced arthritis, *Melicope ptelefolia*, rheumatoid arthritis, synovial fibroblast

Introduction

Rheumatoid arthritis (RA) is a chronic autoimmune disease with an increasing global prevalence (1), characterized by

chronic synovial inflammation, cartilage and joint erosion, pannus formation, joint abnormalities, and ankylosis. Although RA is commonly considered to arise due to exogenous factors (2,3), the exact cause of RA remains to be fully elucidated and as such, there is no known cure (4). Therefore, patients with RA currently require novel therapeutic treatments that can inhibit the inflammation and erosion of joints without any unwanted side effects.

Although the pathogenesis of RA remains to be fully elucidated, pro-inflammatory mediators, including autoantibodies and cytokines, are considered to function within the mechanisms of its expression (5). Autoantibodies secreted by activated B cells and plasma cells target various of the cartilage components affected by RA, which results in the increased autoreactivity of B and T cells and the progression of RA (6). An overproduction of interleukin (IL)-6, tumor necrosis factor (TNF)α, IL-1 and IL-17 is found in the synovial fluid of patients with RA (7). Pro-inflammatory cytokines produced by infiltrated immune cells influence osteoclast formation by upregulating the expression of receptor activator of nuclear factor-κB ligand (RANKL). Increased osteoclast formation may be a factor in the acceleration of bone resorption and thus of RA symptoms (8).

IL-6, a type of pro-inflammatory cytokine, has pleiotropic biological activities and is produced by various types of cells (9). IL-6 stimulates osteoclastogenesis by inducing the expression of RANKL in synovial fibroblasts and osteoblasts (10). Osteoclasts are important in maintaining bone homeostasis through the regulation of bone resorption using proteolytic enzymes and acids. However, an accumulation of IL-6 can lead to the hyperactivation of osteoclasts, which leads to bone and cartilage erosion and ankyloses (11).

Melicope ptelefolia (*M. ptelefolia*) is a dioecious plant that is widespread across Asia, particularly in Malaysia, Vietnam, and southern China. It is a source of 3,5-di-C-β-$_D$-glucopyranosyl phloroacetophenone (βGP). Phytochemical studies have established that acetophenone, benzopyran, bis-isoquinoline alkaloids, and benzopyrans dimers are the main components of *M. ptelefolia* (12,13). *M. ptelefolia* leaves are commonly used not only in the treatment of remittent fever, colds, stomach ache and wounds, but are also used as a natural remedy for rheumatism in certain parts of Asia (14-17). However, several of these reported uses are not substantiated by any published documents, and there are currently few reports on biologically active components of *M. ptelefolia* showing these beneficial effects.

The present study investigated the effects of βGP, a main component of *M. ptelefolia*, on RA and its underlying mechanisms using a mouse model of collagen-induced arthritis (CIA).

Materials and methods

Plant material. The leaves of *M. ptelefolia* were purchased from a market in My Duc herbal distract of Hanoi, Vietnam in March 2014. The sample was botanically identified by Dr Tran The Bach at the Institute of Ecology and Biological Resources (Hanoi, Vietnam). A sample of the voucher (KRIBB 010471) has been deposited in the herbarium of the Korea Research Institute of Bioscience and Biotechnology (Daejeon, Korea).

General experimental procedures for extraction and isolation. 1D and 2D nuclear magnetic resonance (NMR) spectroscopy were performed using the Bruker AVANCE 800 (Bruker Corporation, Billerica, MA, USA) NMR spectrometer with TMS as the internal standard. Thin layer chromatography was performed with silica gel 60 F_{254} and RP-18 F_{254} plates. High-performance liquid chromatography (HPLC) was performed using the Gilson HPLC system with a 321 pump and a UV/VIS-155 detector. An RS Tech Optima Pak C_{18} column (10x250 mm, 5-μm particle size; RStech Corporation, Daejeon, Korea) was used as the HPLC column. ESI-MS data were obtained using Agilent Technologies 6130 Quadrupole liquid chromatography/ionization mass spectrometry (LC/MS). IR spectra (KBr) were obtained using Nicolet 6700 FT-IR (Thermo Fisher Scientific, Inc., Waltham, MA, USA). All solvents used for extraction and isolation were of an analytical grade.

Extraction and isolation of βGP from M. ptelefolia. The air-dried *M. ptelefolia* leaves (1.0 kg) were sonicated with water three times at 2-h intervals. The crude extract (174.2 g) was suspended in water and used for Diaion® HP-20 column chromatography, eluted with water, 40% ethanol and acetone to obtain three fractions, respectively. The 40% ethanol fraction (64.1 g) was pre-isolated on MPLC using RP-C18 (Watcher® Flash Cartridge, 3x15 cm; 40-60-μm particle size), eluting with a stepwise gradient of methanol/H_2O (1:9-1:0) to obtain eight subfractions. βGP-rich fractions 2 and 3 were chromatographed using an RP-C18 (4x40 cm; 75-μm particle size) open column, eluting with 40% methanol. Eluted fraction 3 (8.79 g) was directly purified using the Gilson HPLC system (Optima Pak C18 Column; 10x250 mm, 5-μm particle size, RS Tech Corporation) with a mobile phase of methanol in H_2O containing 0.1% HCO_2H (0-50 min: 15-30% methanol, 51-60 min: 100% methanol); a flow rate of 2 ml/min; and UV detection at 205 and 254 nm to yield βGP (t_R=30 min, 1.90 g).

HPLC analysis of βGP. The βGP was quantified using reversed-phase HPLC with an Agilent series 1260 liquid chromatography, a G1322A vacuum degasser, G1312C binary pump, G1329B autosampler, and G1315D DAD detector, and processed using Agilent ChemStation software (Edition Rev.C.01.05 36; Agilent Technologies GmbH, Waldbronn, Germany). The system used MeCN/H_2O [INNO C18 Column; 4.6x250 mm, 5-μm particle size (RS Tech Corporation); mobile phase acetonitrile in H_2O containing 0.1% HCO_2H (3-15 min: 3-20% MeCN, 15-38 min: 20-100% MeCN); flow rate 0.6 ml/min; UV detection at 254 and 300 nm]. A stock solution of purified βGP was prepared by dissolving 1.00 mg of βGP in 50% DMSO. Five additional calibration levels were prepared by diluting this stock solution with water. The calibration curves were constructed by plotting the peak area ratios via OpenLAB CDS analysis (ChemStation; Agilent Technologies GmbH). A good linearity (correlation coefficient values R^2>0.999) was achieved with a relatively wide concentration ranging between 0.31 and 2.5 μg/ml. The lowest concentration of the working solution was mixed with water to yield a series of diluted concentrations. The limits of detection and quantification under the chromatographic conditions were separately determined at a signal-to-noise ratio of ~2 and 12, respectively.

Animal studies. Eight-week-old male DBA/1 (Orient Bio, Inc., Seongnam, Korea) and ICR (Koatech, Pyeongtaek, Korea) mice (20-25 g) were acclimatized to a 12-h light/dark cycle at 22±2˚C for 2 weeks with unlimited access to food and water in a specific pathogen-free facility. The DAB/1 mice were randomly divided into four groups: i) Normal group (n=4); ii) vehicle group (n=16), treated with 0.5% carboxymethylcellulose; iii) βGP 25 group (n=5), treated with 25 mg/kg βGP; iv) βGP 50 group (n=15), treated with 50 mg/kg βGP. From 3 days prior to the second immunization, βGP was administered daily by oral gavage for 18 days. The concentration of βGP was determined based on the results of preliminary animal experiments. Body weight was measured each day. The ICR mice were randomly divided into six groups (0, 2, 4, 8, 24, and 48 h; n=4-5 for each group) and were administered with a single dose of 50 mg/kg βGP by oral gavage. The plasma and livers were obtained from the ICR mice following the specified time periods (0, 2, 4, 8, 24, or 48 h), and βGP concentration was determined by LC-MS. All mice were sacrificed by CO_2 asphyxiation. All animal experiments were approved by the Institutional Animal Care and Use Committee of the Korea Research Institute of Bioscience and Biotechnology (KRIBB-AEC-18001) and performed in accordance with the Guide for the Care and Use of Laboratory Animals published by the US National Institutes of Health (Bethesda, MD, USA).

Cell culture. RAW 264.7 cells, a murine macrophage cell line, and NIH/3T3 fibroblasts were purchased from the American Type Cell Culture (Manassas, VA, USA). The cells were cultured in Dulbecco's modified Eagle's medium (DMEM; Hyclone; GE Healthcare Life Sciences, Logan, UT, USA) containing 10% fetal bovine serum (FBS; Gibco, Thermo Fisher Scientific, Inc.), 100 U/ml penicillin, and 100 μg/ml streptomycin, in a humidified environment (5% CO_2/95% air) at 37˚C. Mouse embryo fibroblasts (MEFs) were isolated from day 13.5 C57BL/6 mouse embryos. Briefly, the embryos were harvested from the uterus of female 13-14 days after the appearance of the copulation plug. The isolated embryos were transferred to a dish with phosphate buffered saline (PBS), and blood was removed by swirling. The head, limbs, and internal organs of the embryo were removed. The rest of the embryos were placed in the covered dish with 0.25% trypsin buffer, and dissected with scissors. Then, the tissues were minced into pieces of 1-2 mm with a scalpel blade, and placed in the 37˚C tissue culture incubator for 10 min. The cell suspensions were transferred to a 50 ml tube, and DMEM containing 10% FBS was added to inactivate the trypsin. The cell suspension sat for 5 min to allow larger embryo fragments to sink to the bottom the tube. The supernatant consisting of single cells and cell clusters was transferred to a T75 flask, and cultured in DMEM containing 10% FBS, 100 U/ml penicillin, and 100 μg/ml streptomycin, in a humidified environment (5% CO_2/95% air) at 37˚C. The RAW 264.7 cells and MEFs at a density of 500,000 cells in a 6 well plate were pre-treated with different concentrations of βGP for 1 h. The RAW 264.7 cells were then stimulated with lipopolysaccharide (LPS; 100 ng/ml; Sigma, EMD Millipore, Billerica, MA, USA) or PBS for 6 h at 37˚C. The MEF cells were stimulated with TNFα (40 ng/ml; Gibco; Thermo Fisher Scientific, Inc.) or PBS for 6 h at 37˚C. NIH/3T3 fibroblasts at a density of 100,000 cells in a 24 well plate were incubated with different concentrations of βGP for 24 h at 37˚C. Cell viability and proliferation were assessed using a Cell Counting Kit-8 (Dojindo Molecular Technologies, Inc., Rockville, MD, USA) with 2-(2-methoxy-4-nitrophenyl)-3-(4-nitrophenyl)-5-(2,4-disulfophenyl)-2H-tetrazolium monosodium salt. The concentration of βGP used in the experiments was determined based on the results of preliminary *in vitro* experiments.

Induction and clinical assessment of CIA. For the induction of arthritis, bovine type II collagen (Chondrex, Redmond, WA, USA) was dissolved at 2 mg/ml in PBS containing 0.1 M acetic acid and emulsified in an equal volume of 2 mg/ml complete Freund's adjuvant (Chondrex). The mice in the vehicle, βGP 25, and βGP 50 groups were immunized intradermally at the base of the tail with 100 μl of emulsion containing 100 μg bovine type II collagen. The animals were boosted with an intradermal injection 21 days later, using the same procedure. At 7 days following the second immunization, the animals were boosted with an intraperitoneal injection of 40 μg LPS. The mice were assessed for swelling of the paws and a clinical score was assigned. Paw swelling was assessed by measuring the mean thickness of all paws with micrometer calipers. The clinical score was assessed using the following system: 0, normal paw; 1, one toe inflamed and swollen; 2, >1 toe, but not the entire paw inflamed and swollen, or mild swelling of the entire paw; 3, entire paw inflamed and swollen; 4, markedly inflamed and swollen or ankylosed paw (18). Each limb was graded, with a maximum possible score of 16 per animal.

Histopathological analysis. The rear paws of each mouse were collected 35 days following the first immunization. The paws were fixed, decalcified, paraffin-embedded, sectioned (5 μm), and stained with hematoxylin and eosin (H&E), safranin O, or toluidine blue. Images were captured using a light microscope (BX51; Olympus Corporation, Tokyo, Japan). The H&E-stained images were analyzed microscopically for the degree of inflammation and for cartilage and bone erosion, using the following scale: 0, normal synovium; 1, synovial membrane hypertrophy and cell infiltrates; 2, pannus and cartilage erosion; 3, major erosion of cartilage and subchondral bone; 4, loss of joint integrity and ankyloses (19).

Micro-computed tomography (μCT). Images of the rear paw ankle joints of the arthritic vehicle- and βGP-treated mice were captured on day 35 using a Quantum FX imaging system (PerkinElmer, Inc., Waltham, MA, USA). The samples were immersed in 10% formalin.

Measurement of serum anti-type II collagen antibodies immunoglobulin (Ig)G, IgG1, and IgG2a by ELISA. Serum samples were collected at the end of the experiment (day 35) for the determination of IgG, IgG1, and IgG2a antibody levels with three commercially available test kits (Chondrex), according to the manufacturer's protocol. The antibody levels were quantified using seven standard serum samples (0.16-10 ng/ml).

Measurement of serum cytokine levels by ELISA. The serum levels of IL-6, IL-10, and TNF were determined using the BD OptEIA™ set (BD Biosciences, San Diego, CA, USA), according to the manufacturer's protocol.

Reverse transcription-quantitative polymerase chain reaction (RT-qPCR) analysis. The total RNA was isolated from the paw tissues, RAW 264.7 cells or MEFs using TRIzol reagent (Invitrogen, Thermo Fisher Scientific, Inc.), and reverse transcribed using the iScript™ cDNA Synthesis kit (Bio-Rad Laboratories, Inc., Hercules, CA, USA). The cycling conditions were as follows: Priming at 25˚C for 5 min and reverse transcription at 46˚C for 20 min and RT inactivation at 95˚C for 1 min. The resulting cDNA was subjected to RT-qPCR using the StepOnePlus™ Real-Time PCR system (Applied Biosystems, Thermo Fisher Scientific, Inc.) with AccuPower® 2X Greenstar qPCR Master mix (Bioneer Corporation, Daejeon, Korea) according to the manufacturers' protocols. A 10 μl reaction mixture was used for one well, and the composition was as follows: 1 μl cDNA (1 ng/μl), 1 μl primer mixtures (5 ϱmol/l) for target gene, 5 μl AccuPower® 2X Greenstar qPCR Master mix, and 3 μl distilled water. The cycling conditions were as follows: Pre-denaturation at 95˚C for 10 min, followed by denaturation at 95˚C for 10 sec, and annealing and extension at 60˚C for 30 sec, for 45 cycles of amplification. Relative gene expression levels were analyzed using the $2^{-\Delta\Delta Cq}$ method (20), and normalized against the expression of 18S rRNA. The primer sequences used in the experiments are listed in Table I.

Western blot analysis. The paws from the DBA/1 mice were collected at the end of the experiment (day 35). The paw tissues and MEF cells were prepared by homogenization in lysis buffer with a protease inhibitor and phosphatase inhibitor. The protein concentration in the supernatant was measured using the Bradford method. Protein samples (25 μg) were separated by 10% sodium dodecyl sulfate gel electrophoresis and transferred onto a PVDF membrane (EMD Millipore). The membranes were stained with primary antibodies specific to p-STAT3 (S727) (catalogue no. 9134; 1:1,000; Cell Signaling Technology, Inc., Danvers, MA, USA) or STAT3 (catalogue no. 9139; 1:1,000; Cell Signaling Technology, Inc.) overnight at 4˚C. Horseradish peroxidase-conjugated goat anti-rabbit secondary antibodies (catalogue no. 111-035-144; 1:1,000; Jackson ImmunoResearch, West Grove, PA, USA) were then added and incubated for 1 h at room temperature. Following washing with Tris-buffered saline and Tween-20, the bands were detected using EzWestLumi plus (Atto Corporation, Tokyo, Japan).

Statistical analysis. Numerical data are presented as the mean ± standard error of the mean. Comparisons between two groups were performed using a two-tailed Student's *t*-test or Wilcoxon's test. Comparisons of multiple groups were performed using the Tukey-Kramer HSD test following one-way analysis of variance. JMP 5.1 software was used for analysis (SAS Institute, Inc., Cary, NC, USA). $P<0.05$ was considered to indicate a statistically significant difference.

Results

Isolation and structure determination of compound βGP from M. ptelefolia. βGP was isolated from *M. ptelefolia* using the bioactive-guided method. As shown in Fig. 1A, the chemical structure of purified βGP was determined by 1D and 2D NMR spectroscopy and by comparison with its physical-chemical properties of a previously published report (14,15).

βGP: brownish gum; $[\alpha]_D^{20}$ + 56.4 (c 0.3, methanol); UV λ_{max} (methanol) (log ε) (nm) 234 (3.48), 286 (3.49); IR (KBr) ν_{max} 3,354, 1,621, 1,447, 1,277, 1,048 cm^{-1}; ESIMS m/z 475.1 $[M-H_2O + H]^+$, 493.2 $[M + H]^+$, 491.1 $[M-H]^-$; ^{1}H NMR (800 MHz, DMSO-d_6): 9.14 (1H, s, 6-OH), 4.70 (2H, d, J=10.0 Hz, H-1', 1''), 3.60 (4H, m, H-6', 6''), 3.47 (2H, t, J=9.0 Hz, H-2', 2''), 3.33 (2H, t, J = 9.0 Hz, H-4', 4''), 3.25 (4H, m, H-3', 3'', 5', 5''), 2.60 (3H, s, H-8); ^{13}C NMR (200 MHz, DMSO-d_6): 104.8 (C-1), 161.4 (C-2, 6), 104.0 (C-3, 5), 161.3 (C-4), 203.4 (C-7), 33.0 (C-8), 74.6 (C-1', 1''), 72.1 (C-2', 2''), 77.8 (C-3', 3''), 69.2 (C-4', 4''), 81.1 (C-5', 5''), 60.0 (C-6', 6'').

Quantitative analysis of the major compound βGP from M. ptelefolia. Quantitative analysis was performed with >98% purity by HPLC and by 1D and 2D NMR spectroscopy following purification of βGP. HPLC was used to quantitatively analyze βGP in the water extract of *M. ptelefolia* and in the 40% ethanol elute of the HP-20 column using the regression equation ($y=203.8991x - 3.862$, $R^2=0.999$). The UV spectrum of the βGP was set to 300 nm to monitor the phenolic compound. The βGP peak was set by spiking the sample with a reference standard and a comparison of its UV, mass spectrum and retention time. The concentration of βGP in the water extract was found to be 13.3%. Following elution with 40% ethanol using Diaion HP-20 column chromatography, the concentration of βGP was increased to 35.5%.

βGP treatment improves collagen-induced arthritis. The gross score of paw arthritis was significantly reduced from day 32 in the βGP 50 group compared to that of the vehicle group (Fig. 1B). Paw size was also significantly decreased in the βGP 50 group (vehicle group, vs. βGP 50 group=2.94±0.16, vs. 2.30±0.11). However, the severity of arthritis was comparable between the vehicle and βGP 25 groups (Fig. 1B and C). In line with paw diameter, the development of swelling or redness of paws was reduced in the rear paws of the βGP 50 group at day 35 (Fig. 1D). These results suggested that βGP had ameliorative effects on CIA. To identify the presence of βGP in the mice, a single dose of 50 mg/kg βGP was administered by oral gavage to male ICR mice. βGP was identified in the plasma and liver at various time points for 48 h following administration. βGP concentration was determined by LC-MS. βGP was retained in its original structure until ~4 h in the plasma and until ~8 h in the liver (data not shown). The levels of blood biochemical markers were comparable among all groups (Table II) and changes in body weight were similar between groups (data not shown), suggesting that βGP did not evoke significant toxicity.

βGP reduces articular inflammation and injury in CIA mice. As the βGP 25 group did not show any differences compared with the vehicle group, further analysis were performed in the vehicle and βGP 50 groups only. Articular inflammation, cartilage damage, and bone erosion were the typical symptoms (21). In H&E staining, the vehicle group showed synovial membrane hypertrophy with marked infiltration of immune cells and intra-articular pannus formation. These observations were lower in the βGP 50 group (Fig. 2A).

Table I. Sequences of polymerase chain reaction primers used in the present study.

Gene	GenBank accession no.	Primer sequence
Tnfα	NM_013693.3	Forward 5'-TGGCCTCCCTCTCATCAGTT-3'
		Reverse 5'-CCTCCACTTGGTGGTTTGCT-3'
Il-6	NM_031168.2	Forward 5'-TTCCATCCAGTTGCCTTCTTG-3'
		Reverse 5'-GGGAGTGGTATCCTCTGTGAAGTC-3'
Il-10	NM_010548.2	Forward 5'-GGGTTGCCAAGCCTTATCG-3'
		Reverse 5'-TCTCACCCAGGGAATTCAAATG-3'
Lif	NM_008501.2	Forward 5'-GGTGGAGCTGTATCGGATGG-3'
		Reverse 5'-TACTTGTTGCACAGACGGCA-3'
Cd68	NM_001291058.1	Forward 5'-TCACAGTTCACACCAGCTCC-3'
		Reverse 5'-CTTGGACCTTGGACTAGGCG-3'
Cd45	NM_001111316.2	Forward 5'-GACAACCTTCGTGCCCAAAC-3'
		Reverse 5'-TGACGAGTTTACACCGCGA-3'
Trap	NM_001102405.1	Forward 5'-GGAACTTCCCCAGCCCTTAC-3'
		Reverse 5'-AGGTCTCGAGGCATTTTGGG-3'
Oscar	NM_001290377.1	Forward 5'-GTAACGGATCAGCTCCCCAG-3'
		Reverse 5'-TGCAAAACTCATGCCCGGTA-3'
CtsK	NM_007802.4	Forward 5'-TACCCATATGTGGGCCAGGA-3'
		Reverse 5'-TTCAGGGCTTTCTCGTTCCC-3'
Calcr	NM_007588.2	Forward 5'-TAGTTAGTGCTCCTCGGGCT-3'
		Reverse 5'-AGTACTCTCCTCGCCTTCGT-3'
Rankl	NM_011613.3	Forward 5'-AGGCTGGGCCAAGATCTCTA-3'
		Reverse 5'-GTCTGTAGGTACGCTTCCCG-3'
18s rRNA	NR_003278.3	Forward 5'-GACACGGACAGGATTGACAGATTGATAG-3'
		Reverse 5'-GTTAGCATGCCAGAGTCTCGTTCGTT-3'

TNFα, tumor necrosis factor-α; *IL*, interleukin; *LIF*, leukocyte inhibitory factor; *Trap*, tartrate-resistant acid phosphatase; *Oscar*, osteoclast associated receptor; *CtsK*, cathepsin K; *Calcr*, calcitonin receptor; *Rankl*, receptor activator of nuclear factor-κB ligand.

In line with the H&E staining results, the histological scores were significantly reduced in the βGP-treated mice compared with that in vehicle-treated mice (vehicle, vs. βGP 50 group=1.69±0.25, vs. 0.82±0.24; Fig. 2B). To confirm the extent of the cartilage damage, the paw tissues were stained with safranin O and toluidine blue, which identify cartilage proteoglycans and glycosaminoglycans (22). As shown in Fig. 2C and D, no positive regions for safranin O (red staining) or toluidine blue (purple staining) were observed in the vehicle group, but this was markedly recovered by βGP treatment, indicating the protective effects of βGP on CIA. A three-dimensional reconstruction of the tarsal bone using μCT showed decreased bone erosion in the βGP 50 group compared to that in the vehicle group (Fig. 2E). These results suggested that βGP improved CIA via the regulation of inflammation, cartilage injury, and bone erosion in the joints.

βGP does not modulate autoantibody production in CIA mice. Subsequently, how βGP affects inflammatory arthritis in CIA mice was investigated. The increased production of anti-collagen antibodies by the humoral immune system is a crucial factor for inducing RA (23). Therefore, to confirm whether βGP can regulate humoral immunity, the present study analyzed the levels of anti-type II collagen antibody in the plasma of CIA mice using ELISA. The levels of total IgG and its subclasses, IgG1 and IgG2a, did not differ significantly between the vehicle and the βGP 50 groups (Fig. 3). These results suggested that the therapeutic effects of βGP on CIA were not associated to the regulation of autoantibody production.

βGP decreases articular macrophage infiltration and inflammatory cytokine expression in CIA mice. The degree of synovial macrophage infiltration is correlated with the severity of joint erosion in RA (24). Therefore, the present study investigated whether βGP influences articular macrophage infiltration in CIA mice. Gene expression levels of the macrophage marker *Cd68* and leukocyte common antigen *Cd45* were significantly reduced in the paws of the βGP 50 group compared with those of the vehicle group (Fig. 4A). Additionally, the gene expression levels of *IL-6*, leukemia inhibitory factor (*LIF*) and *IL-10* were significantly decreased by βGP treatment. The gene expression of *TNF-α* was also found to be reduced in the paws of the βGP 50 group (Fig. 4B). These results suggested that βGP downregulated macrophage infiltration and the levels of inflammatory cytokines in the paws of CIA mice.

Table II. Effects of βGP on plasma biomarkers in collagen-induced arthritis mice.

Group	ALT (IU/l)	AST (IU/l)	BUN (mg/dl)	CHO (mg/dl)	CK (IU/l)	CREA (mg/dl)	TG (mg/dl)
Vehicle	87.27±13.15	148.00±7.19	15.40±0.42	138.00±2.96	482.42±63.84	0.26±0.01	98.27±8.58
βGP 25	43.54±12.15[a]	123.69±18.98	13.38±0.71[b]	131.00±4.10	219.17±29.85[b]	0.24±0.01	85.31±5.07
βGP 50	82.00±17.91	145.46±17.83	15.00±0.77	133.54±3.28	276.70±61.06[b]	0.22±0.02	96.31±7.02

Grouped quantitative data are presented as the mean ± standard error of the mean (n=10-15/group). Significance was measured via the Tukey-Kramer HSD test following one-way analysis of variance; [b]P<0.05. βGP, 3,5-di-C-β-$_D$-glucopyranosyl phloroacetophenone; ALT, alanine transaminase; AST, aspartate transaminase; BUN, blood urea nitrogen; CHO, cholesterol; CK, creatine kinase; CREA, creatine; TG, triglyceride.

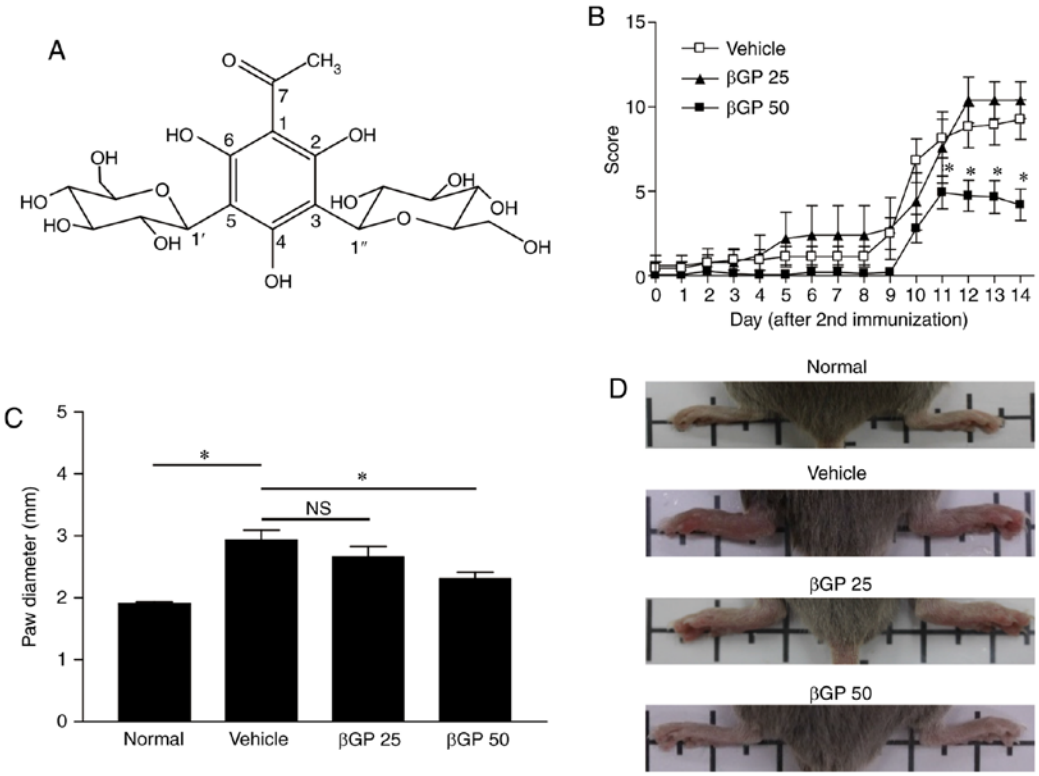

Figure 1. Alleviation of the progression of CIA by administration of βGP. (A) Chemical structure of βGP, isolated from *Melicope ptelefolia*. (B) Mice were intradermally immunized with 100 μg bovine type II collagen and administered with either vehicle, βGP 25, or 50 mg/kg βGP (βGP 50) for 18 days. The clinical arthritis scores were evaluated from 1 day prior to second immunization. (C) Paw diameter in normal and CIA mice at the end of experiment, measured using calipers. (D) Images of the rear paws of normal mice, vehicle-treated mice, and βGP-treated mice. Grouped quantitative data are presented as the mean ± standard error of the mean (normal group, n=4; vehicle group, n=16; βGP 25 group, n=5; βGP 50 group, n=15). Significance was measured using the Tukey-Kramer HSD test following one-way analysis of variance; *P<0.05. CIA, collagen-induced arthritis; βGP, 3,5-di-C-β-$_D$-glucopyranosyl phloroacetophenone; NS, no significant difference; βGP 25, 25 mg/kg GP; βGP 50, 50 mg/kg βGP.

βGP does not affect inflammatory cytokine expression in macrophages. Although macrophages alone do not cause RA, they are important in inflammation and in bone and cartilage erosion (25). The activation and infiltration of macrophages in the joints and in the synovial membrane is crucial for the progression of RA (26). Previous studies and the results of the present study prompted the investigation of the direct effect of βGP on macrophages. To confirm whether βGP can regulate inflammation by controlling macrophages, the LPS-stimulated mouse macrophage cell line, RAW264.7, was treated with βGP. Neither the LPS-induced elevation of gene expression nor protein secretion of cytokines in RAW264.7 cells, except for TNF-α gene expression, was affected by βGP treatment (Fig. 5A and B). This result suggested that βGP does not directly regulate the production of inflammatory cytokines in macrophages.

βGP regulates the expression of RANKL following IL-6 and LIF modulation in fibroblast cells. It has been reported that synovial fibroblasts are a source of inflammatory cytokines and are critical in RA through the regulation of RANKL-mediated osteoclast activation (27). Among cytokines, IL-6 and its family, LIF, regulate the expression of RANKL in synovial fibroblast cells through autocrine or

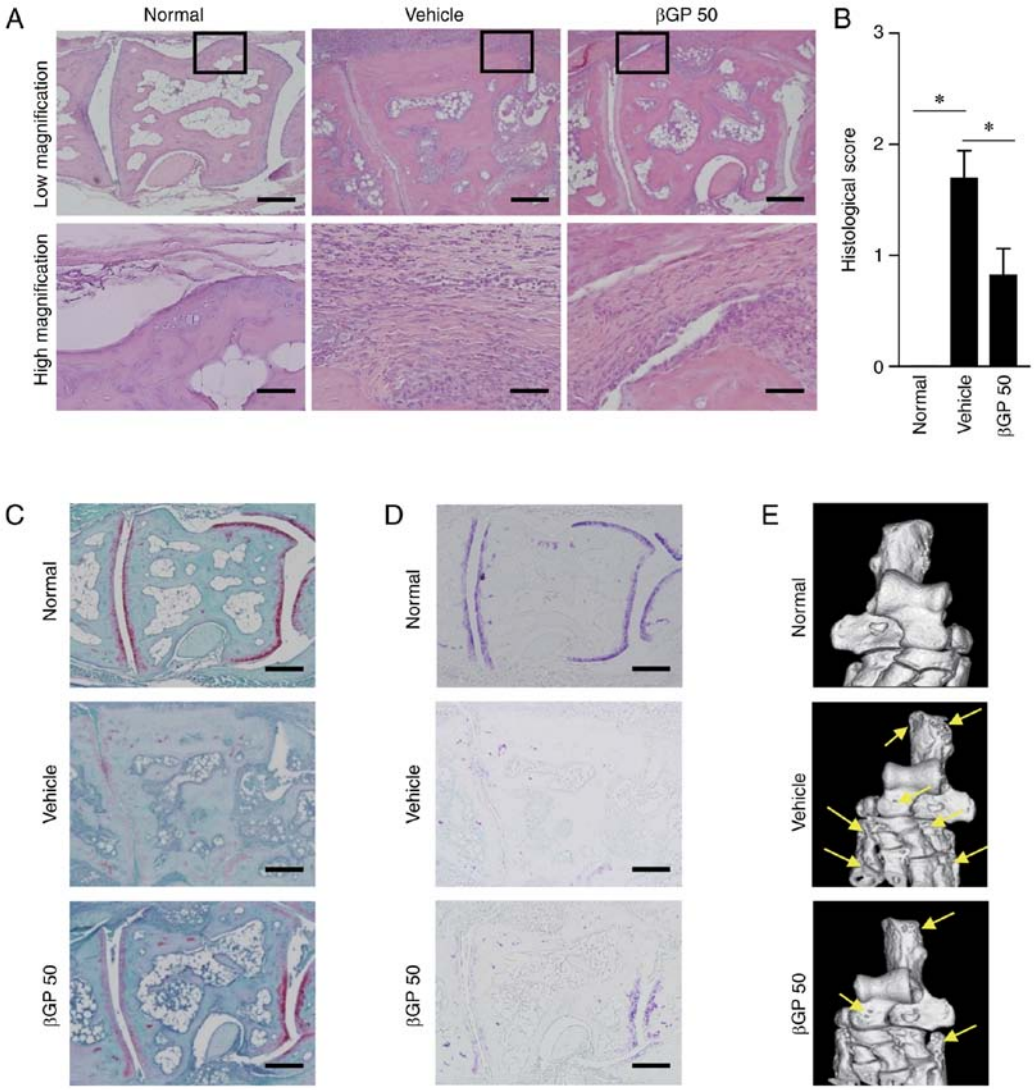

Figure 2. Histological analysis of the anti-arthritic effects of βGP. At 35 days following the first immunization, paws were obtained from all CIA mice treated with either vehicle or βGP. (A) Representative images of mouse paws stained with H&E (scale bar=200 μm). The region outlined with a box in each group is shown at a higher magnification beneath (scale bar=50 μm). (B) Histological scores of the H&E-stained tissues. Representative images of paws stained with (C) safranin O and (D) toluidine blue (scale bar, 200 μm). (E) Representative images of three-dimensional reconstructions of the tarsal bone at 35 days in each group. The arrows point to regions of bone erosion. Grouped quantitative data are presented as the mean ± standard error of the mean (normal group, n=4; vehicle group, n=13; βGP 50 group, n=14). A Wilcoxon test was used to compare the vehicle group with the βGP groups; *P<0.05. CIA, collagen-induced arthritis; βGP, 3,5-di-C-β-$_{D}$-glucopyranosyl phloroacetophenone; βGP 50, 50 mg/kg βGP; H&E, hematoxylin and eosin.

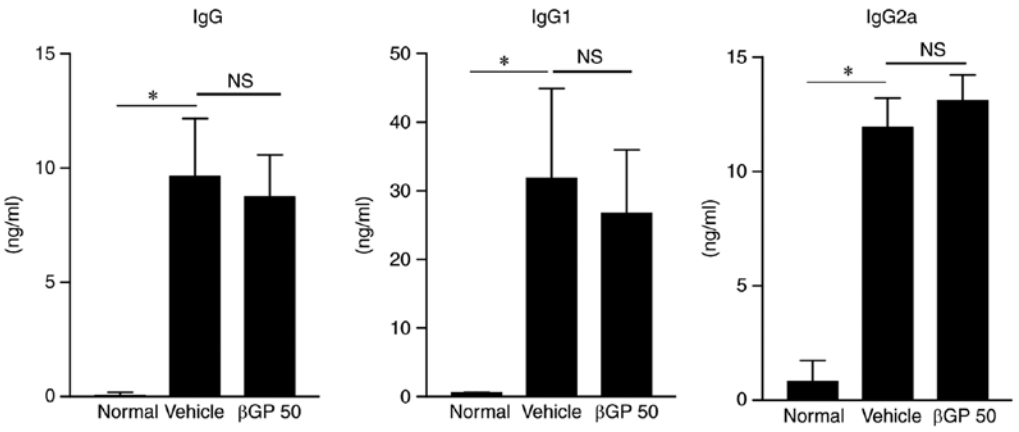

Figure 3. Effect of βGP on the production of anti-type II collagen antibody in serum. The levels of anti-type II collagen IgG and its subtypes were measured using an ELISA assay using plasma obtained at day 35 from each mice group. Grouped quantitative data are presented as the mean ± standard error of the mean (normal group n=4; vehicle group, n=8; βGP 50 group, n=8). Significance was measured using the Tukey-Kramer HSD test following one-way analysis of variance; *P<0.05. βGP, 3,5-di-C-β-$_{D}$-glucopyranosyl phloroacetophenone; βGP 50, 50 mg/kg βGP; Ig, immunoglobulin; NS, no significant difference.

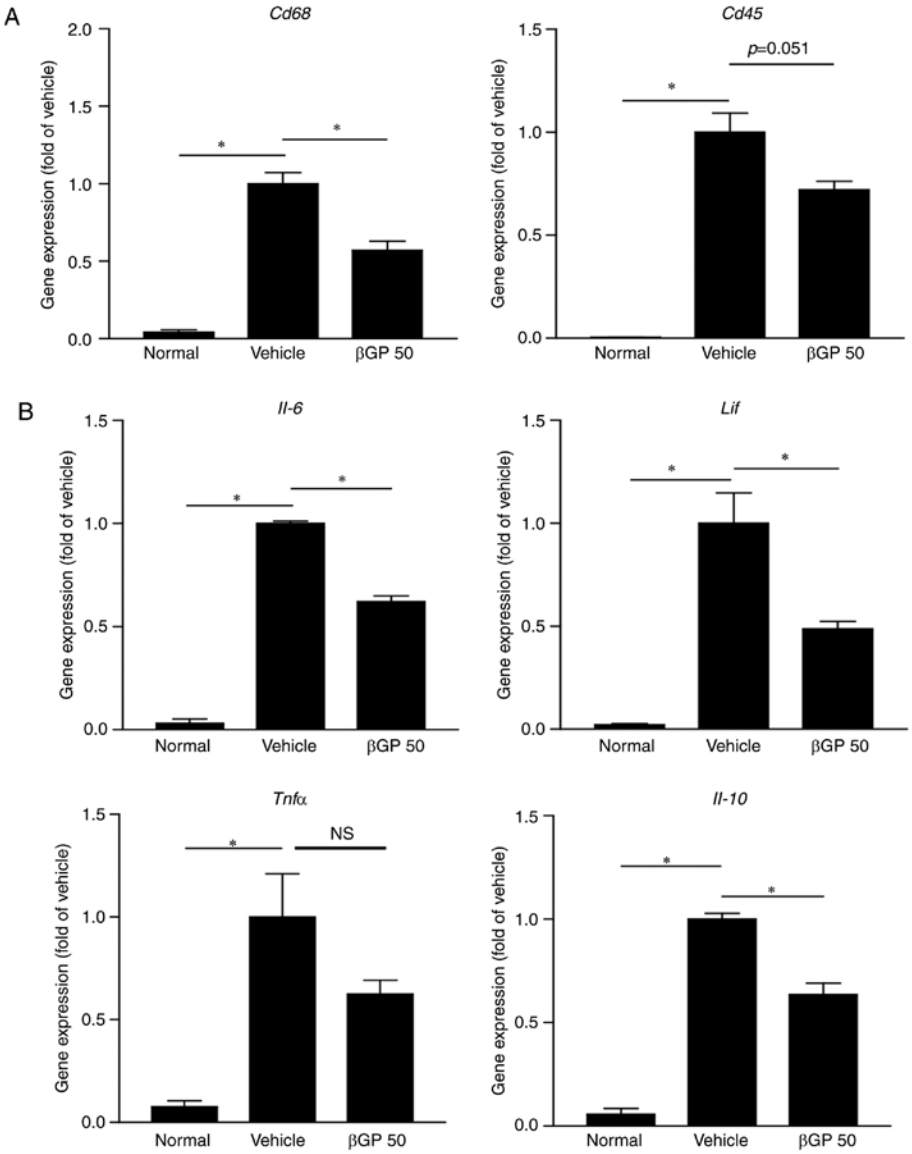

Figure 4. βGP influences gene expression of pro-inflammatory cytokines in CIA mice. At 35 days following the first immunization, paws were obtained from all CIA mice treated with either vehicle or βGP, and gene expression levels were analyzed by reverse transcription-quantitative polymerase chain reaction analysis. (A) Gene expression levels of *Cd68*, a macrophage marker, and *Cd45*, a common leukocyte antigen. (B) Gene expression levels of *IL-6, LIF, TNFα,* and *IL-10*. The vehicle group was set to a value of 1. Its average fold-change is shown. Grouped quantitative data are presented as the mean ± standard error of the mean (normal group, n=4; vehicle group, n=5; βGP 50 group, n=5). Significance was measured using the Tukey-Kramer HSD test following one-way analysis of variance; *P<0.05. CIA, collagen-induced arthritis; βGP, 3,5-di-C-β-$_D$-glucopyranosyl phloroacetophenone; βGP 50, 50 mg/kg βGP; *IL*, interleukin; *LIF*, leukocyte inhibitory factor; *TNFα*, tumor necrosis factor-α; NS, no significant difference.

paracrine modes (27). In addition, IL-6 and LIF-dependent activation of STAT3 is essential for the expression of RANKL in fibroblast cells (27,28). As shown in Fig. 6A and B, the TNFα-stimulated increases in *IL-6* and *LIF* were significantly reduced by βGP co-treatment in MEFs. In addition, βGP markedly reduced the phosphorylation of STAT3 and significantly decreased the gene expression of *RANKL* in the TNFα-treated MEFs (Fig. 6C and D). It has been reported that, in the progression of RA, synovial fibroblasts proliferate, become activated, and invade and destroy adjacent cartilages (29). Therefore, the present study examined the cytotoxicity and effect on cell proliferation of βGP in NIH/3T3 fibroblasts. However, βGP treatment did not induce any significant changes compared with the control group (Fig. 7). These results suggested that βGP may regulate the expression of RANKL through inhibiting the expression of *IL-6* and *LIF* in synovial fibroblast cells.

βGP improves CIA through the regulation of RANKL-dependent osteoclast activation in mice. Periarticular bone erosion and generalized bone loss are hallmarks of RA. It has been reported that osteoclasts, cells specialized in bone resorption, are important for the progression of joint erosion in RA (30). In addition, it is well known that RANKL, an osteoclast activator, is promoted by phosphorylated STAT3 (31). In accordance with the results in the MEFs (Fig. 6), treatment with βGP significantly reduced the phosphorylation of STAT3 and gene expression of *Rankl* in the paws of CIA mice (Fig. 8A and B). Accordingly, osteoclast markers, including tartrate-resistant acid phosphatase, osteoclast associated

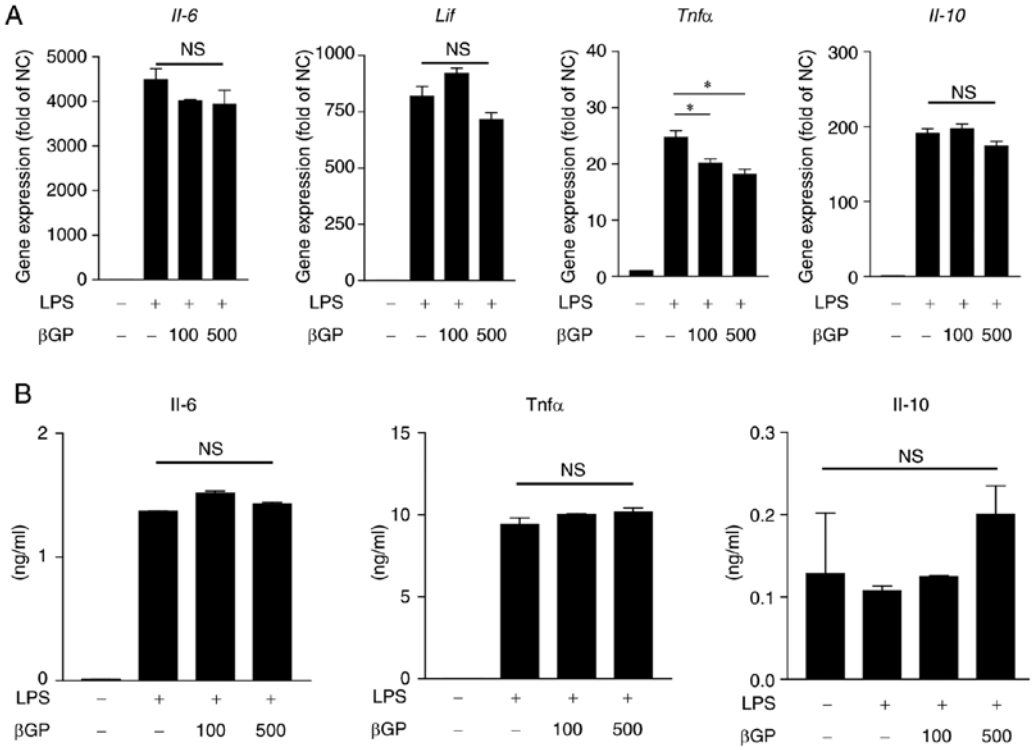

Figure 5. Effects of βGP on pro-inflammatory cytokine changes in LPS-stimulated RAW 264.7 cells. RAW 264.7 cells were pre-treated with different concentrations of βGP (0-500 μg/ml) for 1 h, and stimulated with either 100 ng/ml LPS or vehicle for 6 h. (A) Gene expression levels of *Il-6*, *Lif*, *Tnfα*, and *Il-10* were analyzed by reverse transcription-quantitative polymerase chain reaction analysis. The vehicle group was set to a value of 1. Its average fold-change is shown. (B) Protein levels of IL-6, TNFα, and IL-10 in the cell culture supernatant were measured by ELISA. Grouped quantitative data are presented as the mean ± standard error of the mean (triplicate of RAW264.7 cell lysate cDNA samples and duplicate of RAW264.7 cell culture supernatant). Significance was measured using the Tukey-Kramer HSD test following one-way analysis of variance; *P<0.05. βGP, 3,5-di-C-β-$_D$-glucopyranosyl phloroacetophenone; IL, interleukin; LIF, leukocyte inhibitory factor; TNFα, tumor necrosis factor-α; LPS, lipopolysaccharide; NC, negative control; NS, no significant difference.

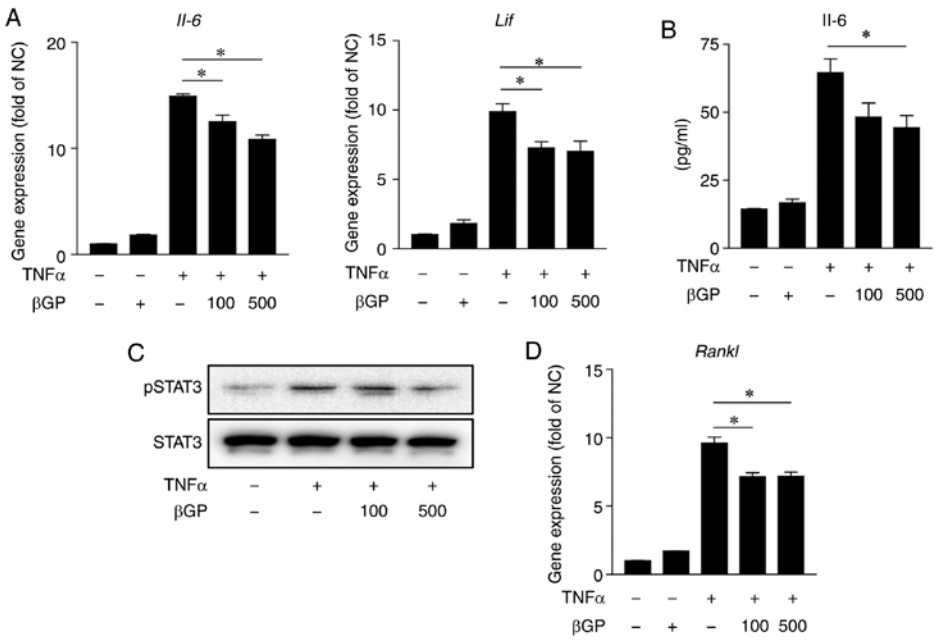

Figure 6. βGP downregulates TNFα-induced inflammation and expression of RANKL in MEFs. MEFs were pre-treated with different concentrations of βGP (0-500 μg/ml) for 1 h and then stimulated with either 40 ng/ml TNFα or vehicle for 6 h. (A) Gene expression levels of *IL-6* and *LIF* were analyzed by RT-qPCR analysis. The vehicle group was set to a value of 1. Its average fold-change is shown. (B) Protein levels of IL-6 in the cell culture supernatant were measured by ELISA. (C) Protein levels of pSTAT3 and STAT3 in the MEF cell lysate were analyzed by western blot analysis. (D) Gene expression levels of *Rankl* were analyzed by RT-qPCR analysis. The vehicle group was set to a value of 1. Its average fold-change is shown. Grouped quantitative data are presented as the mean ± standard error of the mean (triplicate of MEFs lysate cDNA samples and triplicate of MEF cell culture supernatant). Significance was measured using the Tukey-Kramer HSD test following one-way analysis of variance; *P<0.05. βGP, 3,5-di-C-β-$_D$-glucopyranosyl phloroacetophenone; IL, interleukin; LIF, leukocyte inhibitory factor; TNFα, tumor necrosis factor-α; RANKL, receptor activator of nuclear factor-κB ligand; STAT3, signal transducer and activator of transcription 3; pSTAT3, phosphorylated STAT3; MEFs, mouse embryonic fibroblasts; RT-qPCR, reverse transcription-quantitative polymerase chain reaction.

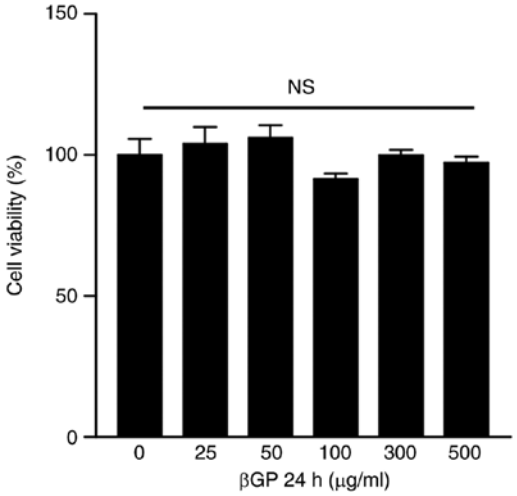

Figure 7. βGP does not show cytotoxicity or a cell proliferation effect in fibroblastic cells. NIH/3T3 fibroblasts were incubated with different concentrations of βGP (0-500 μg/ml) for 24 h. Cell viability and proliferation were determined using a colorimetric cell viability assay kit. Grouped quantitative data are presented as the mean ± standard error of the mean (triplicate of mouse embryo fibroblast cell culture). Significance was measured using the Tukey-Kramer HSD test following one-way analysis of variance. βGP, 3,5-di-C-β-$_D$-glucopyranosyl phloroacetophenone; NS, no significant difference.

receptor, cathepsin K, and calcitonin receptor, were also significantly reduced in the βGP 50 group compared to those in the vehicle group (Fig. 8C). These results suggested that βGP can improve CIA through RANKL-dependent osteoclast regulation.

Discussion

The present study demonstrated the anti-rheumatic potential of βGP as an active compound in the water extract of *M. ptelefolia*. When βGP was administered to CIA mice, their arthritis was significantly relieved, demonstrated by a reduced gross and histologic arthritic score, decreased inflammatory cytokines and expression of RANKL, and decreased expression of osteoclast markers in the paws of mice.

RA is a systemic autoimmune disease characterized by the presence of autoantibodies, and this is used as a diagnostic marker for RA. Autoantibodies not only react with synovial components but also activate T and B cells (6). Cytokines derived from T helper (Th) cells enhance B cell differentiation into Ig-secreting plasma cells and accelerate the production of autoantibodies in patients with RA (32). Among the cytokines, Th2 cytokines regulate the switch from IgM/D to IgG1 and IgE, and Th1 cytokines induce IgG2a secretion in activated B cells (33). In addition, further insight into the importance of B cells in the pathogenesis of RA is highlighted by the efficacy of B cell depletion (34). However, in the present study, the plasma levels of anti-type II collagen autoantibodies, including total IgG, IgG1 and IgG2a, were not altered by the βGP administration in CIA mice. These results demonstrate that the therapeutic effects of βGP were not associated with the modulation of B cell-derived autoantibody regulation in the context of CIA.

Cytokines are directly implicated in several of the immune processes that are associated with the pathogenesis of RA. Numerous cytokines are expressed and are functionally active in the synovial tissues of patients with RA (35). Accordingly, cytokine modulation alters the outcome of several RA rodent models (36). Of note, TNF is targeted in the standard treatment of patients with RA, and other cytokines, including the IL-6 family (IL-6 and LIF), are also being investigated as targets in the clinic, with promising results (37,38). In the present study, βGP decreased the expression levels of *TNFα*, *IL-6* and *LIF* in the paws of CIA mice. Of note, the expression of *IL-10* was also reduced by βGP administration, however, it was interpreted that the expression of *IL-10* may have decreased subsequent to the βGP-mediated amelioration of articular inflammation. These results suggest that βGP can improve RA through the modulation of inflammatory cytokine levels in the joints.

It has been reported that cytokines derived from macrophages and synovial fibroblasts, including TNFα and IL-6, respectively, are important in RA pathogenesis (39). In the present study, to identify a specific target cell of βGP, the effects of βGP on an LPS-treated macrophage cell line and TNFα-stimulated MEFs were examined. βGP did not regulate inflammatory cytokine levels in macrophages following LPS treatment. However, *IL-6* and *LIF* were significantly decreased by βGP treatment in the TNFα-stimulated MEFs. These results suggested that the inhibitory effects of βGP on cytokine production in synovial fibroblasts may partially result in decreased levels of cytokines in the paws of CIA mice. Although βGP did not regulate the production of inflammatory cytokines in macrophages *in vitro*, macrophage markers were markedly reduced by βGP treatment in the paws of CIA mice. These results suggested that the reduction of cytokines in the paws of βGP-treated mice was not solely dependent on the direct modulation of synovial fibroblasts and may result from a decrease of infiltrated macrophages in the joints of CIA mice. Further investigations are required to elucidate the effects of βGP on macrophage migration into the joints of CIA mice and its mechanism of action.

The compound βGP has a similar structure to aspirin, which was derived from willow *(Salix)* bark and is one of the most ideal drugs. Unlike aspirin, which has an acetyl group at position 2, βGP has two sugars at positions 3 and 5, which gives βGP a higher polarity than aspirin. In addition, the presence of the two sugars in βGP is considered to be non-absorbable through the brain barrier as a larger molecule. Therefore, the effects of βGP may be driven not by central nervous system regulation, but by peripheral nervous system modulation, considering the targeted mechanism of βGP through the local mode of action of aspirin. The principle mechanism considered to be responsible for the anti-inflammatory effects of aspirin is the inhibition of cyclooxygenase (COX)-dependent prostaglandin (PG) synthesis (40). It has been reported that aspirin inhibits the secretion of IL-6 through COX-dependent PG regulation in adipose tissue (41). In addition, TNFα accelerates the transactivation and COX-2 increases PG release in human gingival fibroblasts (42). Taken together, it is possible that aspirin regulates TNFα-stimulated IL-6 induction via the downregulation of COX-dependent PG synthesis in nonimmune cells. In the present study, the gene expression of *Tnfα* was markedly increased in the paws of CIA mice, compared with that in normal mice. Although the elevated level of TNFα was similar between the vehicle and βGP groups, the level of

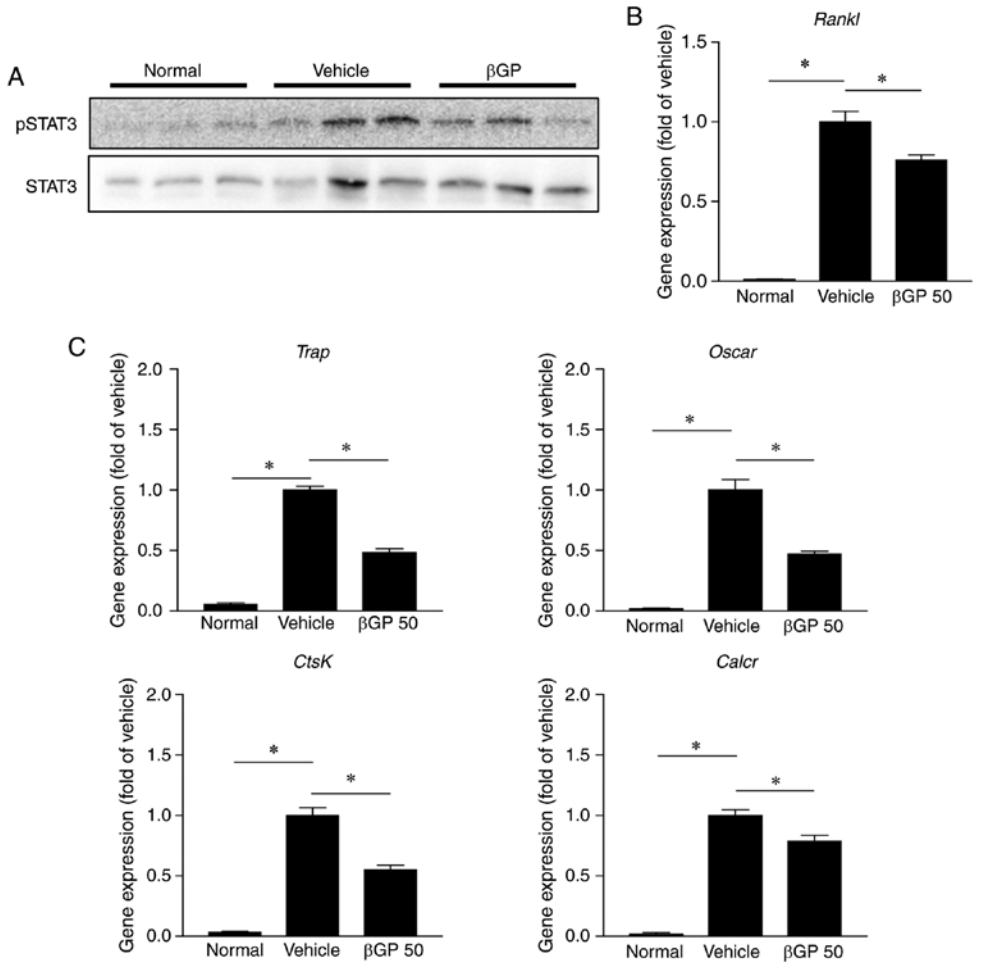

Figure 8. βGP influences osteoclast activity in CIA mice. At 35 days following the first immunization, paws were obtained from each CIA mouse treated with either vehicle or βGP. (A) Protein levels of pSTAT3 and STAT3 in the paw were analyzed by western blot analysis. (B) Gene expression levels of *Rankl* in the paw were analyzed by RT-qPCR analysis. The vehicle group was set to a value of 1. Its average fold-change is shown. (C) Gene expression levels of osteoclast activity markers in the paw were analyzed by RT-qPCR analysis. The vehicle group was set to a value of 1. Its average fold-change is shown. Grouped quantitative data are presented as the mean ± standard error of the mean (normal group, n=4; vehicle group, n=5; βGP 50 group, n=5). Significance was measured using the Tukey-Kramer HSD test following one-way analysis of variance; $^{*}P<0.05$. βGP, 3,5-di-C-β-$_{D}$-glucopyranosyl phloroacetophenone; STAT3, signal transducer and activator of transcription 3; pSTAT3, phosphorylated STAT3; *Rankl*, receptor activator of nuclear factor-κB ligand; *Trap*, tartrate-resistant acid phosphatase; *Oscar*, osteoclast associated receptor; *CtsK*, cathepsin K; *Calcr*, calcitonin receptor.

Il-6 was significantly reduced by βGP administration in the paw. In addition, βGP treatment significantly decreased the expression of IL-6 in the TNFα-stimulated MEFs and in the paws of CIA mice. Although the exact mechanism of βGP in CIA was not confirmed, the aspirin-like skeleton characteristics in compound βGP suggested the possibility that βGP may target and inhibit the COX-induced upregulation of PG and the subsequent downregulation of IL-6.

Osteoclasts are terminally differentiated cells of the monocyte/macrophage lineage that resorb bone matrix. Bone destruction in RA is mainly attributable to the abnormal activation of osteoclasts (43). Osteoclast formation, activation and survival are mainly regulated by RANKL (44). Among the cytokines, IL-6 and LIF upregulate the expression of RANKL in RA synovial fibroblasts through the Janus kinase 2/STAT3 signaling pathway (45,46). Therefore, osteoclast regulation via inhibiting STAT3-dependent expression of RANKL is an efficient way to treat RA (47,48). In the present study, βGP significantly reduced the expression levels of IL-6 and LIF in TNFα-stimulated MEFs and in the paws of CIA mice. Furthermore, phosphorylated STAT3 and the expression of RANKL were significantly reduced by βGP treatment, followed by decreased expression levels of osteoclast markers. These results suggest that βGP modulates osteoclast activity via regulation of the STAT3-dependent expression of RANKL in the paws of CIA mice.

In terms of βGP metabolism *in vivo*, the present study found that βGP remained until ~4 h and 8 h in the plasma and the liver. Although detailed analysis of βGP metabolism was not performed, the results suggested the possible rapid metabolism of this compound. Future investigations aim to further elucidate the metabolism of βGP.

In conclusion, the present study is the first study, to the best of our knowledge, to demonstrate that the compound βGP had therapeutic effects against RA in mice. βGP suppressed osteoclasts by reducing the STAT3-mediated induction of RANKL following inhibition of the expression of IL-6 and LIF in synovial fibroblasts. The results of the present study provide novel insights into the possibility of βGP and *M. ptelefolia* active fraction applications as therapeutics to prevent RA.

Acknowledgements

The authors would like to thank Mr. I.B. Lee, Mr. Y.K. Choi, Mrs. Y.J. Seo and Mrs. J.H. Choi (Laboratory Animal Resource Centre, Korea Research Institute of Bioscience and Biotechnology, Daejeon, Korea) for their technical assistance.

Funding

This study was supported by grants from the Korea Bioactive Natural Material Bank (grant no. NRF-2017M3A9B8069409) and the Bio & Medical Technology Development Program (grant no. NRF-2016K1A1A8A01939075) of the National Research Foundation, which were funded by the Korean government (Ministry of Science and ICT) and from the KRIBB Research Initiative Program of the Republic of Korea.

Availability of data and materials

The datasets generated in the present study are not currently available to the public but will be available from the corresponding author upon reasonable request.

Authors' contributions

HJK, CHL, WKO, and YHK designed the experiments and the study. HJK, JHC, DHC, SWK, JYL, JGP, and YHK collected the data and performed experiments for the study. HJK, JRN, SJM, HYK, SWK, JYL, JGP, and YHK analyzed the data. JHH, KSK, SC, SME, TTB, JR, SRO, and CHL provided critical revisions to the text. All authors read and approved the final manuscript.

Ethics approval and consent to participate

All animal experiments were approved by the Institutional Animal Care and Use Committee of the Korea Research Institute of Bioscience and Biotechnology (KRIBB-AEC-18001) and were performed in accordance with the Guide for the Care and Use of Laboratory Animals published by the US National Institutes of Health.

Patient consent for publication

Not applicable.

Competing interests

The authors declare that they have no competing interests.

References

1. Myasoedova E, Crowson CS, Kremers HM, Therneau TM and Gabriel SE: Is the incidence of rheumatoid arthritis rising? Results from olmsted county, minnesota, 1955-2007. Arthritis Rheum 62: 1576-1582, 2010.
2. Jiang SH, Ping LF, Sun FY, Wang XL and Sun ZJ: Protective effect of taraxasterol against rheumatoid arthritis by the modulation of inflammatory responses in mice. Exp Ther Med 12: 4035-4040, 2016.
3. Xu H, Wang J, Wang C, Chang G, Lin Y, Zhang H, Zhang H, Li Q and Pang T: Therapeutic effects of micheliolide on a murine model of rheumatoid arthritis. Mol Med Rep 11: 489-493, 2015.
4. Choy E: Understanding the dynamics: Pathways involved in the pathogenesis of rheumatoid arthritis. Rheumatology (Oxford) 5 (Suppl 51): v3-v11, 2012.
5. Shin JS, Yun CH, Chung KS, Bang MH, Baek NI, Chung HG, Cho YW and Lee KT: Standardized ethyl acetate fraction from the roots of brassica rapa attenuates the experimental arthritis by down regulating inflammatory responses and inhibiting NF-κB activation. Food Chem Toxicol 66: 96-106, 2014.
6. Song YW and Kang EH: Autoantibodies in rheumatoid arthritis: Rheumatoid factors and anticitrullinated protein antibodies. QJM 103: 139-146, 2010.
7. Hashizume M, Hayakawa N and Mihara M: IL-6 trans-signalling directly induces RANKL on fibroblast-like synovial cells and is involved in RANKL induction by TNF-alpha and IL-17. Rheumatology (Oxford) 47: 1635-1640, 2008.
8. Weitzmann MN: The role of inflammatory cytokines, the RANKL/OPG axis, and the immunoskeletal interface in physiological bone turnover and osteoporosis. Scientifica (Cairo) 2013: 125705, 2013.
9. Srirangan S and Choy EH: The role of interleukin 6 in the pathophysiology of rheumatoid arthritis. Ther Adv Musculoskelet Dis 2: 247-256, 2010.
10. Kwan Tat S, Padrines M, Théoleyre S, Heymann D and Fortun Y: IL-6, RANKL, TNF-alpha/IL-1: Interrelations in bone resorption pathophysiology. Cytokine Growth Factor Rev 15: 49-60, 2004.
11. Charles JF and Aliprantis AO: Osteoclasts: More than 'bone eaters'. Trends Mol Med 20: 449-459, 2014.
12. Kamperdick C, Van NH, Sung TV and Adam G: Benzopyrans from *Melicope ptelefolia* leaves. Phytochemistry 45: 1049-1056, 1997.
13. Hong Van N, Kamperdick C, Van Sung T and Adam G: Benzopyran dimers from *Melicope ptelefolia*. Phytochemistry 48: 1055-1057, 1998.
14. Nguyen NH, Ha TK, Choi S, Eum S, Lee CH, Bach TT, Chinh VT and Oh WK: Chemical constituents from *Melicope pteleifolia* leaves. Phytochemistry 130: 291-300, 2016.
15. Sulaiman MR, Mohd Padzil A, Shaari K, Khalid S, Shaik Mossadeq WM, Mohamad AS, Ahmad S, Akira A, Israf D and Lajis N: Antinociceptive activity of *Melicope ptelefolia* ethanolic extract in experimental animals. J Biomed Biotechnol 2010: 937642, 2010.
16. Loi DT: Nhung cay Thuoc va vi thuoc Viet Nam (Glossary of Vietnamese Medicinal Plants). Science and Technics Publication, Hanoi, Vietnam, 1977.
17. Perry LM and Metzger J: Medicinal Plants of East and Southeast Asia: Attributed Properties and Uses. MIT Press, Cambridge, UK, 1980.
18. Lee CH, Bae SJ and Kim M: Mucosa-associated lymphoid tissue lymphoma translocation 1 as a novel therapeutic target for rheumatoid arthritis. Sci Rep 7: 11889, 2017.
19. Sun J, Jia Y, Li R, Guo J, Sun X, Liu Y, Li Y, Yao H, Liu X, Zhao J and Li Z: Altered influenza virus haemagglutinin (HA)-derived peptide is potent therapy for CIA by inducing Th1 to Th2 shift. Cell Mol Immunol 8: 348-358, 2011.
20. Livak KJ and Schmittgen TD: Analysis of relative gene expression data using real-time quantitative PCR and the 2(-Delta Delta C(T)) method. Methods 25: 402-408, 2001.
21. Schett G and Gravallese E: Bone erosion in rheumatoid arthritis: Mechanisms, diagnosis and treatment. Nat Rev Rheumatol 8: 656-664, 2012.
22. Schmitz N, Laverty S, Kraus VB and Aigner T: Basic methods in histopathology of joint tissues. Osteoarthritis Cartilage 3 (Suppl 18): S113-S116, 2010.
23. van Boekel MA, Vossenaar ER, van den Hoogen FH and van Venrooij WJ: Autoantibody systems in rheumatoid arthritis: Specificity, sensitivity and diagnostic value. Arthritis Res 4: 87-93, 2002.
24. Yanni G, Whelan A, Feighery C and Bresnihan B: Synovial tissue macrophages and joint erosion in rheumatoid arthritis. Ann Rheum Dis 53: 39-44, 1994.
25. Kinne RW, Bräuer R, Stuhlmüller B, Palombo-Kinne E and Burmester GR: Macrophages in rheumatoid arthritis. Arthritis Res 2: 189-202, 2000.
26. Davignon JL, Hayder M, Baron M, Boyer JF, Constantin A, Apparailly F, Poupot R and Cantagrel A: Targeting monocytes/macrophages in the treatment of rheumatoid arthritis. Rheumatology (Oxford) 52: 590-598, 2013.
27. Baumann H and Kushner I: Production of interleukin-6 by synovial fibroblasts in rheumatoid arthritis. Am J Pathol 152: 641-644, 1998.

28. Palmqvist P, Persson E, Conaway HH and Lerner UH: IL-6, leukemia inhibitory factor, and oncostatin M stimulate bone resorption and regulate the expression of receptor activator of NF-kappa B ligand, osteoprotegerin, and receptor activator of NF-kappa B in mouse calvariae. J Immunol 169: 3353-3362, 2002.
29. Ospelt C: Synovial fibroblasts in 2017. RMD Open 3: e000471, 2017.
30. Durand M, Boire G, Komarova SV, Dixon SJ, Sims SM, Harrison RE, Nabavi N, Maria O, Manolson MF, Mizianty M, *et al*: The increased in vitro osteoclastogenesis in patients with rheumatoid arthritis is due to increased percentage of precursors and decreased apoptosis-the In vitro osteoclast differentiation in arthritis (IODA) study. Bone 48: 588-596, 2011.
31. Hikata T, Takaishi H, Takito J, Hakozaki A, Furukawa M, Uchikawa S, Kimura T, Okada Y, Matsumoto M, Yoshimura A, *et al*: PIAS3 negatively regulates RANKL-mediated osteoclastogenesis directly in osteoclast precursors and indirectly via osteoblasts. Blood 113: 2202-2212, 2009.
32. Cope AP, Schulze-Koops H and Aringer M: The central role of T cells in rheumatoid arthritis. Clin Exp Rheumatol 25 (Suppl 46): S4-S11, 2007.
33. Kaplan C, Valdez JC, Chandrasekaran R, Eibel H, Mikecz K, Glant TT and Finnegan A: Th1 and Th2 cytokines regulate proteoglycan-specific autoantibody isotypes and arthritis. Arthritis Res 4: 54-58, 2002.
34. Edwards JC, Szczepanski L, Szechinski J, Filipowicz-Sosnowska A, Emery P, Close DR, Stevens RM and Shaw T: Efficacy of B-Cell-targeted therapy with rituximab in patients with rheumatoid arthritis. N Engl J Med 350: 2572-2281, 2004.
35. Brennan F and Foey A: Cytokine regulation in RA synovial tissue: Role of T cell/macrophage contact-dependent interactions. Arthritis Res 3 (Suppl 4): S177-S182, 2002.
36. Alves CH, Farrell E, Vis M, Colin EM and Lubberts E: Animal models of bone loss in inflammatory arthritis: From cytokines in the bench to novel treatments for bone loss in the bedside-a comprehensive review. Clin Rev Allergy Immunol 51: 27-47, 2016.
37. Siebert S, Tsoukas A, Robertson J and McInnes I: Cytokines as therapeutic targets in rheumatoid arthritis and other inflammatory diseases. Pharmacol Rev 67: 280-309, 2015.
38. St C: Interleukin 10 treatment for rheumatoid arthritis. Ann Rheum Dis 58 (Suppl 1): I99-I102, 1999.
39. Brzustewicz E and Bryl E: The role of cytokines in the pathogenesis of rheumatoid arthritis-practical and potential application of cytokines as biomarkers and targets of personalized therapy. Cytokine 76: 527-536, 2015.
40. Vane JR: Inhibition of prostaglandin synthesis as a mechanism of action for aspirin-like drugs. Nat New Biol 231: 232-235, 1971.
41. Ogston NC, Karastergiou K, Hosseinzadeh-Attar MJ, Bhome R, Madani R, Stables M, Gilroy D, Flachs P, Hensler M, Kopecky J and Mohamed-Ali V: Low-dose acetylsalicylic acid inhibits the secretion of interleukin-6 from white adipose tissue. Int J Obes (Lond) 32: 1807-1815, 2008.
42. Nakao S, Ogtata Y, Shimizu E, Yamazaki M, Furuyama S and Sugiya H: Tumor necrosis factor alpha (TNF-alpha)-induced prostaglandin E2 release is mediated by the activation of cyclo-oxygenase-2 (COX-2) transcription via NFkappaB in human gingival fibroblasts. Mol Cell Biochem 238: 11-18, 2002.
43. Jones DH, Kong YY and Penninger JM: Role of RANKL and RANK in bone loss and arthritis. Ann Rheum Dis 2 (Suppl 61): ii32-ii39, 2002.
44. Feng X: RANKing intracellular signaling in osteoclasts. IUBMB Life 57: 389-395, 2005.
45. Boyce BF and Xing L: Functions of RANKL/RANK/OPG in bone modeling and remodeling. Arch Biochem Biophys 473: 139-146, 2008.
46. Tawara K, Oxford JT and Jorcyk CL: Clinical significance of interleukin (IL)-6 in cancer metastasis to bone: Potential of anti-IL-6 therapies. Cancer Manag Res 3: 177-189, 2011.
47. Miyamoto T, Mori T, Yoshimura A and Toyama T: STAT3 is critical to promote inflammatory cytokines and RANKL expression in inflammatory arthritis. Arthritis Res Ther 14 (Suppl 1): P43, 2012.
48. O'Brien CA, Gubrij I, Lin SC, Saylorsi RL and Manolagas SC: STAT3 activation in stromal/osteoblastic cells is required for induction of the receptor activator of NF-κB ligand and stimulation of osteoclastogenesis by gp130-utilizing cytokines or interleukin-1 but not 1,25-dihydroxyvitamin d3 or parathyroid hormone. J Biol Chem 274: 19301-19308, 1999.